The Plant Journal (2008) **53**, 352–367 doi: 10.1111/j.1365-313X.2007.03344.x

Not all ALMT1-type transporters mediate aluminum-activated organic acid responses: the case of *ZmALMT1* – an anion-selective transporter

Miguel A. Piñeros[1,†,*], Geraldo M. A. Cançado[2,†,‡], Lyza G. Maron[1], Sangbom M. Lyi[1], Marcelo Menossi[2] and Leon V. Kochian[1,*]
[1]*United States Plant, Soil, and Nutrition Laboratory, United States Department of Agriculture-Agricultural Research Service, Cornell University, Ithaca, NY 14853-2901, USA, and*
[2]*Laboratório de Genômica Funcional, Centro de Biologia Molecular e Engenharia Genética, Universidade Estadual de Campinas, Campinas, São Paulo 13083-970, Brazil*

Received 26 July 2007; revised 25 September 2007; accepted 28 September 2007.
[*]For correspondence (fax +1 607 255 2459; e-mail map25@cornell.edu or lvk1@cornell.edu).
[†]These authors contributed equally to this paper.[‡]Present address: Empresa de Pesquisa Agropecuária de Minas Gerais (EPAMIG), Belo Horizonte 31170-000, Brazil.

Summary

The phytotoxic effects of aluminum (Al) on root systems of crop plants constitute a major agricultural problem in many areas of the world. Root exudation of Al-chelating molecules such as low-molecular-weight organic acids has been shown to be an important mechanism of plant Al tolerance/resistance. Differences observed in the physiology and electrophysiology of root function for two maize genotypes with contrasting Al tolerance revealed an association between rates of Al-activated root organic acid release and Al tolerance. Using these genotypes, we cloned *ZmALMT1*, a maize gene homologous to the wheat *ALMT1* and Arabidopsis *AtALMT1* genes that have recently been described as encoding functional, Al-activated transporters that play a role in tolerance by mediating Al-activated organic acid exudation in roots. The *ZmALMT1* cDNA encodes a 451 amino acid protein containing six transmembrane helices. Transient expression of a *ZmALMT1*::GFP chimera confirmed that the protein is targeted to the plant cell plasma membrane. We addressed whether *ZmALMT1* might underlie the Al-resistance response (i.e. Al-activated citrate exudation) observed in the roots of the Al-tolerant genotype. The physiological, gene expression and functional data from this study confirm that *ZmALMT1* is a plasma membrane transporter that is capable of mediating elective anion efflux and influx. However, gene expression data as well as biophysical transport characteristics obtained from *Xenopus* oocytes expressing *ZmALMT1* indicate that this transporter is implicated in the selective transport of anions involved in mineral nutrition and ion homeostasis processes, rather than mediating a specific Al-activated citrate exudation response at the rhizosphere of maize roots.

Keywords: aluminum toxicity, aluminum tolerance, ALMT, root exudates, transporter protein, *Zea mays*.

Introduction

Crop plant species undergo a dramatic loss in yield when grown on acidic soils (pH < 5.0), mainly due to the presence of a phytotoxic form of aluminum (Al^{3+}) that is solubilized at low soil pH values. Fortunately, plant species have evolved diverse mechanisms to overcome this stress, either by preventing Al^{3+} from entering root cells (resistance mechanisms) or by increasing their tolerance to Al as it is absorbed and acquired by the root systems (tolerance mechanisms). The basis of these Al resistance and tolerance mechanisms has been the focus of intense research (for recent reviews, see Kochian *et al.*, 2004, 2005). Although a number of possible physiological Al resistance and tolerance mechanisms have been proposed and studied over the years, the most compelling experimental evidence supports the existence of resistance mechanisms based on chelation of Al at the root surface. This is accomplished via exudation of organic acids from the root, which prevents Al from entering the root. Exudation of di- and tricarboxylic acids such as citrate, malate and/or oxalate at the root surface (and into root apoplastic spaces) in response to Al stress immobilizes Al^{3+}

by forming stable, non-toxic complexes. Although Al-activated root malate release in wheat is by far the most extensively characterized Al exclusion mechanism, high levels of Al-activated malate, citrate and oxalate release have also been correlated with differential Al tolerance in a number of monocot and dicot species (see Table I in Kochian *et al.*, 2004). Al resistance cannot entirely be explained by Al-activated organic release in species such as maize (Piñeros *et al.*, 2005). Nonetheless, Al tolerance is strongly associated with high citrate exudation rates from the roots of Al-tolerant varieties of this species (Jorge and Arruda, 1997; Kollmeier *et al.*, 2001; Mariano and Keltjens, 2003; Pellet *et al.*, 1995; Piñeros *et al.*, 2002, 2005).

Anion channels play a significant role in several plant stress responses (see recent review by Roberts, 2006). In the case of Al resistance, as organic acids exist in the cytoplasm primarily as anions, the thermodynamics of organic acid efflux suggest that membrane channels are likely to mediate the efflux of organic acids as they move down a steep, outwardly directed electrochemical gradient. In fact, endogenous currents mediated by anion channels that are specifically activated by extracellular Al^{3+} have been identified in protoplasts isolated from root tips of Al-resistant wheat (Ryan *et al.*, 1997; Zhang *et al.*, 2001) and maize (Kollmeier *et al.*, 2001; Piñeros and Kochian, 2001; Piñeros *et al.*, 2002). The transport and activation properties of these channels are similar to those of the Al-activated malate and citrate exudation observed in wheat and maize intact roots, respectively. Recently, a novel type of membrane transporter (aluminum-activated malate transporter, *ALMT1*) was cloned from wheat (Sasaki *et al.*, 2004), and subsequently shown to confer increased Al tolerance in roots of transgenic barley plants (Delhaize *et al.*, 2004). In addition, *ALMT1* is strongly expressed in the root tips of Al-tolerant wheat lines (Sasaki *et al.*, 2004), and the protein has been shown to be localized to the plasma membrane (Yamaguchi *et al.*, 2005). These findings, in conjunction with genetic mapping data showing that *ALMT1* co-localizes with a major Al tolerance locus (Raman *et al.*, 2005), suggest that *ALMT1* is a major Al tolerance gene in wheat, possibly encoding the Al^{3+}-activated transporter electrophysiologically characterized in protoplasts from Al-tolerant wheat lines. Recently, *ALMT1* homologues from Arabidopsis (*AtALMT1*) and rape (*BnALMT1* and *BnALMT2*) were also shown to encode Al-activated malate transporters that mediate Al-activated malate exudation in roots, and quite likely play an important role in the Al tolerance response in these plant species (Hoekenga *et al.*, 2006; Ligaba *et al.*, 2006). Given that Al-activated malate exudation in wheat, rape and Arabidopsis has been shown to be mediated by ALMT1-type transporters, and that Al^{3+}-activated endogenous anion transporters similar to those described in wheat protoplasts have also been recorded in maize protoplasts, it is reasonable to speculate that a homologue of *ALMT1* may be involved in Al-activated root citrate release in maize.

In this work, we describe the characterization of an *ALMT1* homologue in maize, *ZmALMT1*. We present physiological, molecular and functional evidence suggesting that, although *ZmALMT1* encodes a transporter capable of mediating anion-selective influx and efflux, the maize ZmALMT1 is not likely to mediate the specific Al-activated citrate exudation observed in maize roots under Al stress, in contrast to the Al-activated malate transporters described in wheat, rape and Arabidopsis. In fact, its functional and expression characteristics suggest that ZmALMT1 quite probably plays a role in anion mineral nutrition and general anion homeostasis *in planta*.

Results

Whole-plant Al stress physiology

The contrasting degree of Al tolerance exhibited between the two maize genotypes used in this study was correlated with physiological mechanisms known to facilitate Al exclusion from the root apex. Root growth of Cateto 100-6 (Cat100-6, Al-tolerant) was relatively insensitive to the presence of external Al^{3+}, showing only a 20% reduction (relative to the control) within a 5-day period (Figure 1a). In contrast, S1587-17 (Al-sensitive) showed an increasingly strong inhibition of root growth (40% of control within the first day), which resulted in complete arrest of root development by the end of the 5-day period. The higher degree of Al tolerance in Cat100-6 relative to S1587-17 was associated with higher rates of Al-activated citrate exudation from the root apex (Figure 1b), substantiating the association between rates of citrate exudation and Al tolerance. High levels of citrate exudation probably lead to the chelation of Al^{3+} at the rhizosphere, resulting in lower rates of Al uptake into the root apoplasm and symplasm. These results are in agreement with the fact that Al accumulation in the root apices was significantly lower in Cat100-6 than in S1587-17 (Figure 1c). The whole-root physiological observations described for these two maize genotypes are in agreement with previous results suggesting that Al exclusion mediated by Al-activated root organic acid exudation is a potential mechanism of Al resistance in maize (Jorge and Arruda, 1997; Mariano and Keltjens, 2003; Pellet *et al.*, 1995; Piñeros *et al.*, 2002, 2005).

Al-induced changes in resting membrane potentials in Cat100-6 and S1587-17 roots

As changes in resting membrane potential (E_m) are a function of the overall flux of charged molecules (e.g. organic anions) across the plasma membrane, the short-term effects of Al on the electrical properties of the plasma membrane of

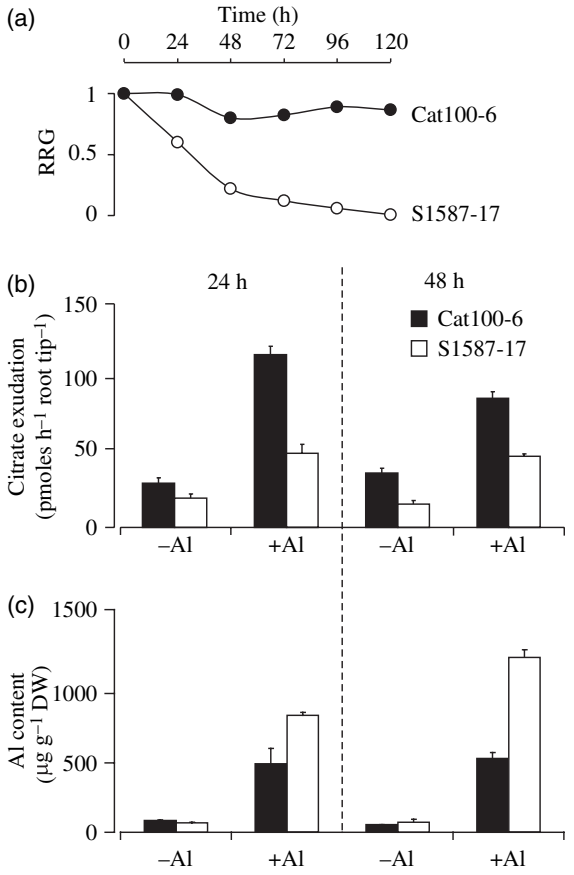

Figure 1. Contrasting levels of Al resistance exhibited by maize genotypes Cat100-6 (filled symbols) and S1587-17 (open symbols).
(a) Relative root growth (RRG) of seedlings grown in nutrient solution containing 39 μM Al^{3+} activity over a 5-day period (n = 20 root measurements).
(b) Citrate exudation rates from the apical root region (first 10 mm of root apices) of the two maize genotypes measured after 24 and 48 h of exposure to 0 or 39 μM Al^{3+} activity. (n = 6).
(c) Al content in the root apical region (first 10 mm) of the two maize genotypes after 24 and 48 h of exposure to 0 or 39 μM Al^{3+} activity.
Values are means ± SEM.

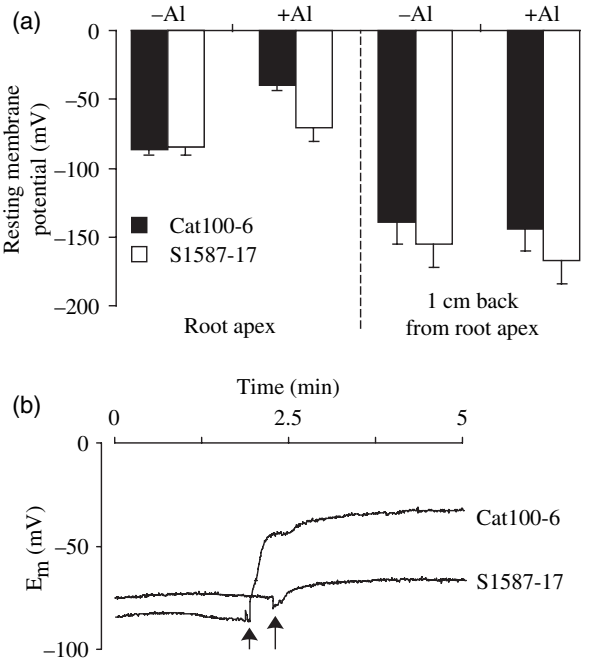

Figure 2. Effects of Al on the resting membrane potential (E_m) of root cells of maize genotypes Cat100-6 and S1587-17.
(a) Resting membrane potentials in the presence of a total Al concentration of 0 or 150 μM $AlCl_3$ (90 μM Al^{3+} activity) measured at two sites along the root (root apex and 10 mm back from the tip). Measurements of at least 18 independent roots were performed for each treatment.
(b) Representative traces showing Al-induced changes in membrane potentials of root apex cells from each maize genotype. An arrow indicates the time at which the control solution was replaced by an identical solution containing 150 μM $AlCl_3$.

root cells from both maize genotypes were examined by characterizing the changes in E_m prior to and upon exposure to Al (Figure 2). Changes in E_m were recorded at two sites along the root: the root apex and 10 mm back from the apex. There were no significant differences in the magnitude of the resting membrane potentials recorded for the two genotypes in the absence of Al at either root site. However, E_m values recorded for root apical cells of both genotypes were consistently less negative than those recorded in cells located 10 mm back from the apex (approximately −85 mV compared with −150 mV). The E_m of mature root cells did not change with the addition of Al (90 μM Al^{3+} activity) to the external solution. In contrast, addition of Al led to fast depolarization of the plasma membrane in cells of the root apex in both genotypes (Figure 2b). The magnitude of the Al-induced membrane depolarization observed in apical cells from Cat100-6 roots was significantly greater (about 45 mV) than that recorded in root apex cells from S1587-17 (about 15 mV): external Al led to a 50% reduction in the E_m of Cat100-6 root apex cells compared to a 10% reduction observed in cells from S1587-17. As the apex cells are probably more susceptible to damage during the impalement process due to their small size, the specificity of the depolarization response was verified by recording the changes in E_m elicited by La^{3+}, a trivalent analogue of Al^{3+}. Exposure to concentrations of La^{3+} in the bath medium identical to those for Al^{3+} resulted in a depolarization that was smaller (14 ± 4 mV) than those recorded in response to Al^{3+} in root apex cells of Cat100-6, while the depolarization in S1587-17 was similar to that elicited by Al (8 ± 3 mV, data not shown). The latter results corroborate the conclusion that the depolarization responses are specific to the presence of extracellular Al^{3+}. Furthermore, membrane recordings in the presence of identical Al activities to those used to measure citrate exudation over a longer time period (39 μM Al^{3+}; Figure 1) resulted in a similar, but less pronounced, membrane depolarization pattern. Exposure to 39 μM Al^{3+}

resulted in a depolarization of 16 ± 2 mV in apical cells from Cat100-6 roots, in contrast to the lack of change (i.e. −2 ± 5 mV) in E_m observed in apical cells from S1587-17 (data not shown). Likewise, the E_m of mature root cells from both genotypes remained relatively unchanged (depolarizations of −6 ± 2 and −6 ± 4 mV) upon exposure to 39 μM Al^{3+} activity. In summary, Cat100-6 root cells showed a root apex-specific, Al-induced membrane depolarization that was significantly greater than that observed in cells from the same root region of S1587-17. These results suggest that differences in transport rates and/or transport properties exist between these two maize genotypes. The large Al-activated depolarization in the root apex of Al-tolerant Cat100-6 is consistent with Al activating a large anion efflux (such as efflux of citrate anions).

Cloning of ZmALMT1*, an* ALMT1 *homologue from maize*

Wheat ALMT1 and Arabidopsis AtALMT1, members of the aromatic acid efflux family of transporters, have recently been shown to mediate the Al-activated organic acid efflux response in wheat and Arabidopsis roots. As wheat ALMT1 is also permeable to citrate when expressed in *Xenopus* oocytes (Sasaki *et al.*, 2004), it is reasonable to assume that a homologous protein could underlie similar processes in maize, and thus account for the whole-root and electrophysiological responses to Al described above. In order to identify *ALMT1* homologues in maize, the wheat *ALMT1-1* ORF was used as a query in TBLASTX searches against the maize genome assembly database (version 3.1 contigs; http://www.plantgenomics.iastate.edu/maize). The search returned a total of six MAGI (maize assembled genomic island) sequences with some degree of similarity to *ALMT1* (local alignment e-values <1e-30), among which MAGI_92675 showed the highest degree of similarity (e-value 1e-123). While MAGI_92675 shared a high degree of similarity to *ALMT1* throughout the entire ORF sequence, careful analysis of the BLAST alignments revealed that the high degree of similarity to *ALMT1* displayed by the other five MAGIs was restricted to short regions of the sequences (results not shown). Wheat *ALMT1-1* was also used as a query in a search against the maize EST database (http://www.plantgdb.org/PlantGDB-cgi/blast/index.cgi). A total of three putative unique transcripts that showed significant similarity to *ALMT1* were identified, among which the contig PUT-157a-Zea_mays-022741 (plant GDB-assembled unique transcript) showed the highest degree of similarity to *ALMT1* (e-value 1e-51). A sequence alignment revealed that this EST is in fact the transcript produced by the gene contained in MAGI_92675 (mentioned above), as the two sequences are 100% identical except for the portions of the MAGI corresponding to the introns.

The results of these searches indicated that MAGI_92675 carries a gene that is probably the closest maize homologue

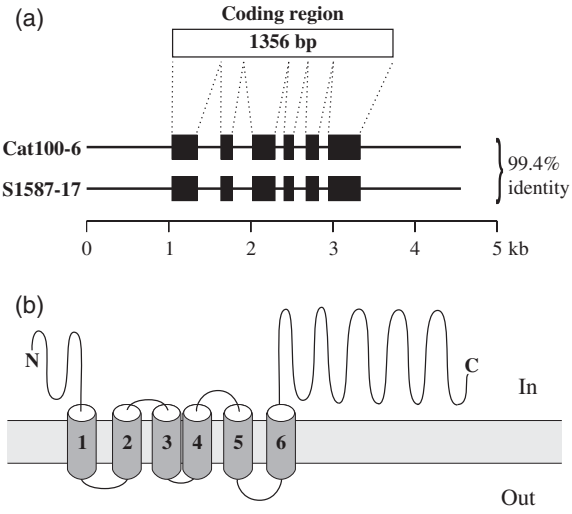

Figure 3. Structure of *ZmALMT1* and of its predicted protein.
(a) Representation of the intron/exon structure of *ZmALMT1* within the genomic region sequenced from maize genotypes Cat100-6 (Al-resistant) and S1587-17 (Al-sensitive). Predicted exons are represented by black bars.
(b) Structural prediction of the ZmALMT1 protein, showing the six transmembrane domains as predicted by HMMTOP (Tusnady and Simon, 2001).

to wheat *ALMT1* (based on the sequences available), and, more importantly, which has been shown to be actively transcribed in maize tissues (based on the presence of an EST sequence). Therefore, this gene is a possible candidate for a maize *ALMT1* homologue, which we now refer to as *ZmALMT1* (*Zea mays ALMT1* homologue 1).

A genomic region of approximately 4.5 kb containing the coding region of *ZmALMT1* was cloned from Cat100-6 and S1587-17, and sequenced. The sequences obtained from both genotypes showed 99.4% identity throughout the entire genomic region (Figure 3a), while the Cat100-6 genomic sequence showed 98% identity to MAGI_92675 (sequenced from maize genotype B73). Comparison of the full-length *ZmALMT1* cDNA with genomic sequences indicated that the *ZmALMT1* gene consists of six exons encoding a 451 amino acid protein. The predicted secondary structure of *ZmALMT1* consists of six transmembrane helices (Figure 3b). Within the coding region, one non-conserved polymorphism was observed between Cat100-6 and S1587-17, causing a Pro to Leu amino acid substitution at position 368. This non-conserved polymorphism is found in what is predicted to be the long hydrophilic tail, and does not affect the transmembrane structure prediction of the protein. Figure 4 illustrates the amino acid sequence alignment of *ZmALMT1* and those *ALMT1* homologues from other plant species that have been functionally characterized. *ZmALMT1* shares significant amino acid identity (58%) and similarity (67%) to wheat *ALMT1*. In contrast, the Arabidopsis and rape homologues showed significantly lower amino acid identity (30 and 33%, respectively) and

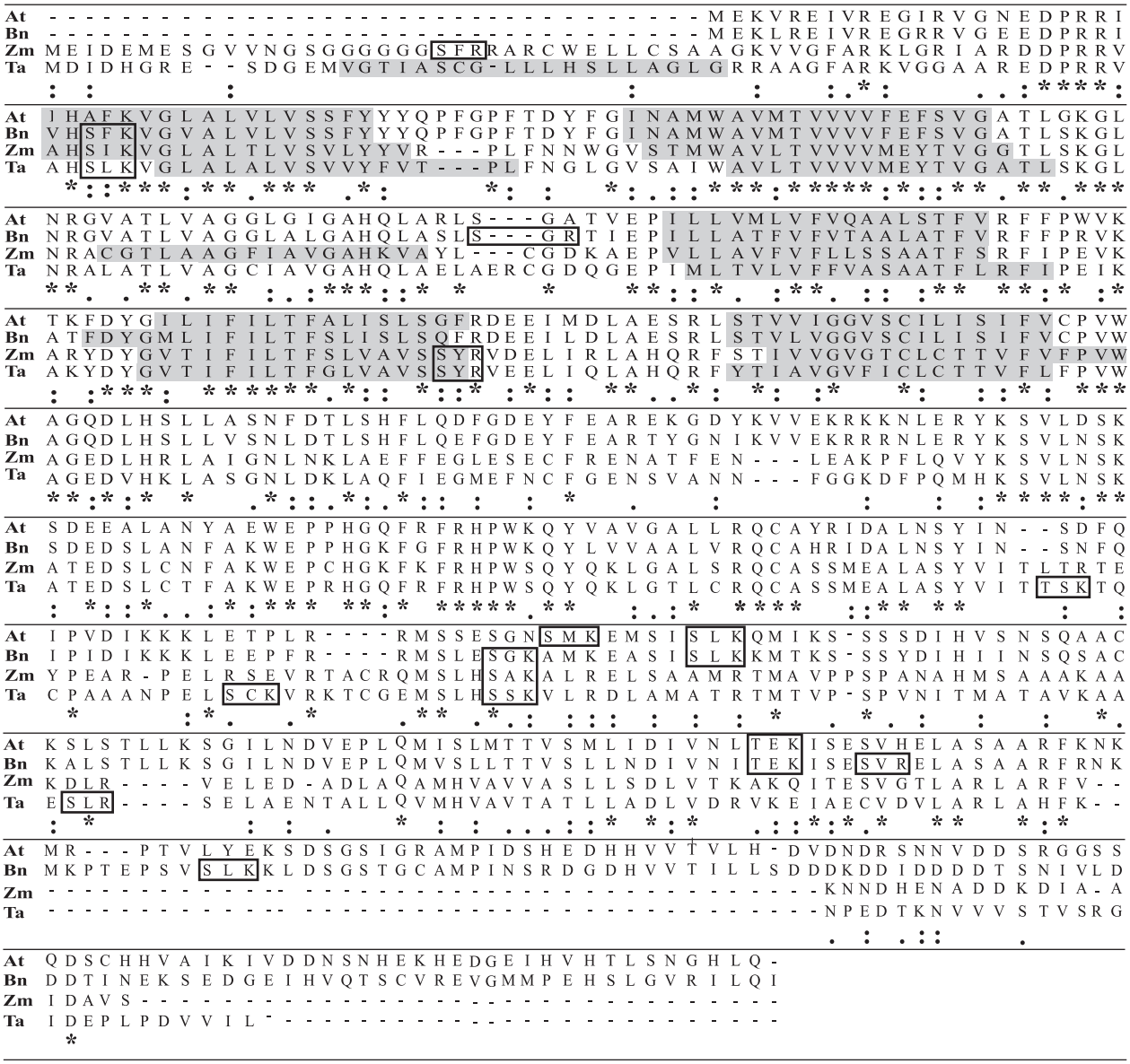

Figure 4. Amino acid sequence alignment for maize *ZmALMT1* (*Zm*, accession number DQ358745), wheat *ALMT1* (*Ta*, accession number AB081803), Arabidopsis *AtALMT1* (*At*, accession number NM100716) and rape *BnALMT1* (*Bn*, accession number AB194301).
The symbols under the sequence alignment indicate identical residues (*), and strongly conserved (:) and weakly conserved (.) substitutions according to the BLOSUM62 matrix. Amino acids belonging to a given transmembrane segment (TMS) are shaded in gray. Alignments and TMS predictions are based on CLUSTALW and HMMTOP routines run on TMS align Biotool (http://saier-144–37.ucsd.edu/tms_align.html). The location of the putative protein kinase C phosphorylation motifs (indicated by boxes) was determined using PROSITE (Rost *et al.*, 2003).

similarity (43%) to *ZmALMT1*, respectively. Comparison of the transmembrane domain predictions for these ALMT1-type proteins indicates that the four transporters have an N-terminus region consisting of at least five common membrane-spanning domains; the maize protein (ZmALMT1) and wheat protein (TaALMT1) are predicted to have one additional transmembrane region. Presumably, this region containing the membrane-spanning domains is responsible for forming the pore structure (i.e. permeation pathway) of the protein. This region is followed by a long hydrophilic C-terminal tail in all four transporters. Additionally, four predicted phosphorylation sites for protein kinase C were identified in the ZmALMT1 sequence, of which three (excluding the first one) are also present in AtALMT1.

Cellular localization of ZmALMT1::*GFP*

The cellular localization of ZmALMT1 protein was investigated using transient expression assays of a translational fusion with green fluorescent protein (GFP) in a

heterologous system. For this purpose, a *ZmALMT1*::GFP chimera was transiently expressed in onion epidermal cells using particle bombardment (Figure 5). In control cells (i.e. transformed with empty vector), GFP fluorescence was observed in the nucleus and cytosol (Figure 5a–d). In contrast, in cells transformed with the *ZmALMT1*::GFP construct, green fluorescence was associated with the cell periphery, presumably due to localization to the plasma membrane (Figure 5i–l). Cell plasmolysis confirmed that the fluorescence in cells expressing ZmALMT1::GFP was localized to the plasma membrane (Figure 5m–p). In plasmolysed control cells, GFP fluorescence was clearly associated with the cell nucleus and cytosol (Figure 5e–h). These results strongly suggest that ZmALMT1 is localized to the plasma membrane, as is its wheat homologue (Yamaguchi *et al.*, 2005). In addition, these findings are consistent with the secondary structure predictions showing that ZmALMT1 is a transmembrane protein.

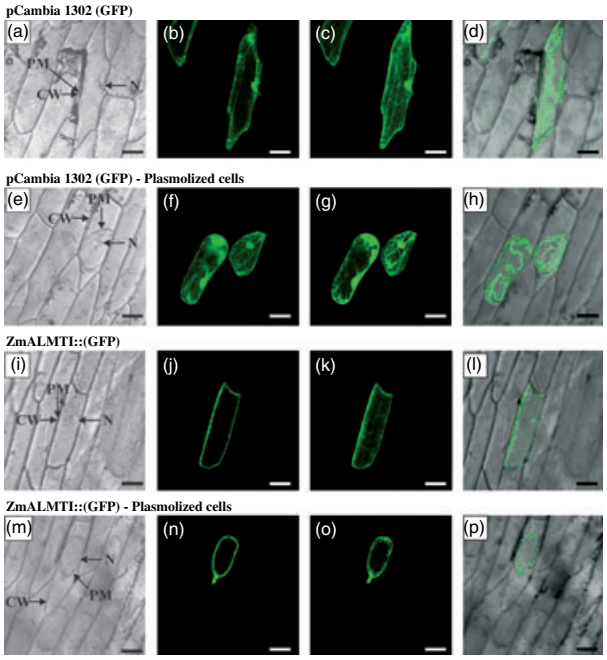

Figure 5. Membrane localization of ZmALMT1 protein in epidermal onion cells.
The top two rows show GFP fluorescence patterns of cells transformed with the pCAMBIA1302 empty vector as a negative control, prior to (a–d) and following (e–h) cell plasmolysis. The third and fourth rows show GFP fluorescence patterns for cells transformed with the *ZmALMT1*::GFP chimera prior to (i–l) and following (m–p) cell plasmolysis. Cell plasmolysis was achieved by incubating onion epidermal strips in 1 M sucrose solution for 10 min. Bright-field images indicating cellular structures (PM, plasma membrane; CW, cell wall; N, nucleus) are shown in the first column (a, e, i, m). Detection of GFP fluorescence is shown in the second column (b, f, j, n). The third column (c, g, k, o) shows average fluorescence signals of 20 section Z-series images obtained at 1 μm intervals from the same specimens shown in the second column. The fourth column (d, h, l, p) shows an overlay of the bright-field and fluorescence images in the first and third columns. Scale bar = 50 μm. Images are representative of four independent replicate experiments.

ZmALMT1 *expression in Cat100-6 and S1587-17*

The expression of *ZmALMT1* was evaluated using semi-quantitative RT-PCR. As the root apex has been shown to be the primary target of Al toxicity and the site where Al-activated citrate exudation rates differ between the two maize genotypes evaluated in the present study (Figures 1 and 2), we investigated the effects of Al on the expression of *ZmALMT1* in root tips. Constitutive expression levels in root tips of both Cat100-6 and S1587-17 were similarly low (Figure 6a). In contrast, exposure to increasing concentrations of Al^{3+} resulted in strong up-regulation of *ZmALMT1* expression in the root tips of both maize genotypes (Figure 6b). Although expression levels in the Al-sensitive genotype tended to be slightly higher under Al^{3+} conditions than those detected in the Al-tolerant genotype, these differences could not be correlated with the differences in transport properties observed between root apical cells from the two genotypes (i.e. Figures 1 and 2), suggesting that ZmALMT1 is unlikely to underlie them. To further evaluate the potential role of ZmALMT1, we analyzed its constitutive expression in other plant tissues. Expression of *ZmALMT1* in the rest of the root and in the shoot showed higher constitutive levels than in root tips, with no apparent differences between the expression levels found in the two genotypes tested (Figure 6b). Although tissue specificity is not a conclusive indicator of functional roles, these results do suggest that ZmALMT1 may play a more significant role in ion transport and homeostasis in other parts of the plant than at the root tip. Nonetheless, although the expression levels were similar in root tips of the sensitive and tolerant genotypes, given that *ZmALMT1* expression does undergo an increase in root tips upon exposure to Al, without

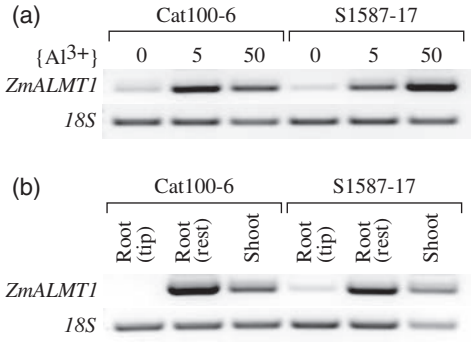

Figure 6. Expression profile of *ZmALMT1* in various tissues of Cat100-6 and S1587-17 determined using semi-quantitative RT-PCR.
(a) *ZmALMT1* expression in root tips exposed to Al^{3+} activity of 0, 5 or 50 μM for 24 h.
(b) Constitutive expression in root tips (10 mm), the rest of the root (rest) and shoots.
The bottom panels show expression of ribosomal 18S used as a loading control. Data shown are representative of two independent biological replicates.

any knowledge of its functional properties, its role in Al-activated root tip citrate exudation could not be entirely ruled out.

Functional characterization of ZmALMT1 in Xenopus laevis *oocytes*

To further address the potential role of ZmALMT1 *in planta*, we examined the electrophysiological properties of the protein and compared them to what has been previously described for its homologues in wheat, Arabidopsis and rape. For this purpose, *ZmALMT1* was expressed in *X. laevis* oocytes, and its functional properties were characterized using two-electrode voltage clamp (TEVC) techniques (Figure 7). First, we compared the net currents of control oocytes with those of oocytes expressing *ZmALMT1*, under ionic conditions in which Al^{3+} was absent or present in the bath medium. In the absence of Al^{3+}, control cells showed no significant inward current (i.e. negative current, which represents net cation influx or anion efflux) and a small, time-dependent outward current (i.e. positive current) (Figure 7a, left panel). Addition of Al^{3+} to the bath medium resulted in inhibition of this outward current. In contrast, in the absence of Al^{3+}, cells expressing ZmALMT1 showed large inward and outward currents that were significantly greater than those elicited in control cells using identical voltage protocols (Figure 7a, right panel). Addition of Al^{3+} to the bathing solution only slightly enhanced the magnitude of the inward current, and had no significant effect on the magnitude of the outward current mediated by ZmALMT1. Figure 7(b) shows the average steady-state current/voltage relationships (*I*/*V*) obtained for the recordings described above. Examination of the time-dependent kinetics of the inward currents mediated by ZmALMT1 revealed some degree of current inactivation (Figure 7c), similar to that previously described for the Arabidopsis ALMT1 homologue AtALMT1 (Hoekenga *et al.*, 2006). However, in contrast to AtALMT1, the inactivation kinetics of the inward currents mediated by ZmALMT1 (Figure 7a–c) showed an additional, unique 'fingerprint', such that the currents elicited at voltages close to −120 mV inactivated more slowly than currents elicited at membrane potentials that were more negative or positive than this value. This response was further characterized by analyzing the kinetics of the current inactivation (Figure 7d). The currents elicited between −130 and −90 mV had significantly slower inactivation time constants compared to those elicited at more negative or more positive test potentials. This phenomenon, unique to ZmALMT1, results in the 'indentation' of the current/voltage relationship observed at around −100 mV (see arrow in Figure 7b). These observations suggest that, in addition to a quite small Al^{3+}-regulatory response (e.g. mild enhancement of transport activity), ZmALMT1 transport activity can also be partially controlled by the voltage across the membrane.

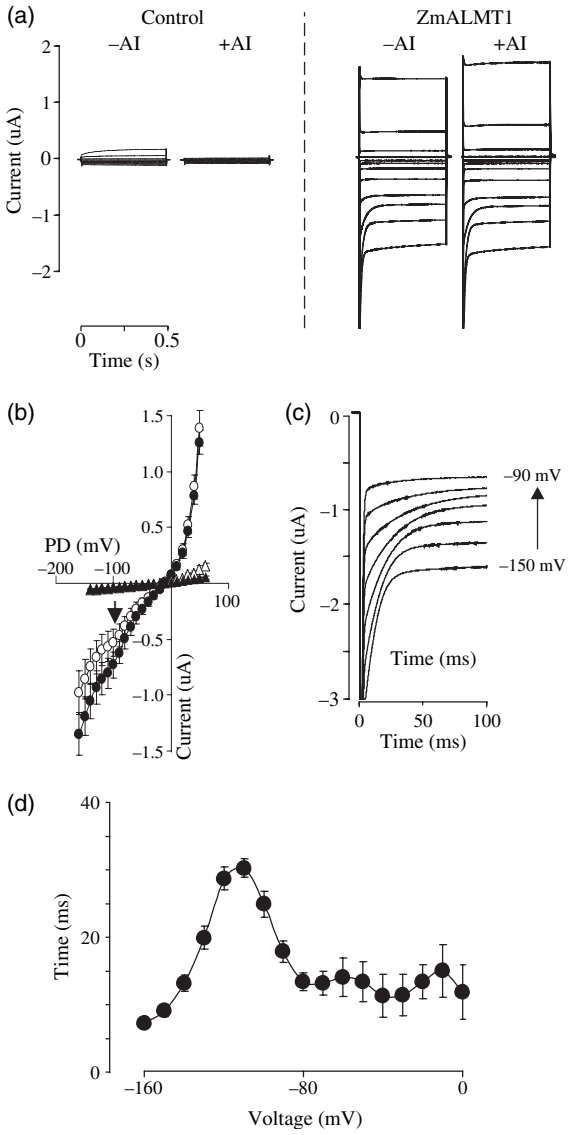

Figure 7. Electrophysiological characterization of ZmALMT1 in *Xenopus laevis* oocytes in ND96 (see Experimental procedures for detailed ionic composition).

(a) Example of ZmALMT1-mediated currents in oocytes in the absence (left panel) and presence (right panel) of Al^{3+}. The holding potential was set to 0 mV and voltage pulses were stepped between −160 and +50 mV (in 10 mV increments). A 10 sec resting interval was allowed between successive voltage steps. For clarity, only currents in response to 20 mV steps are displayed. Currents elicited in control cells (i.e. not injected with cRNA) under both ionic conditions (minus and plus Al^{3+}) are shown on the left of each panel.

(b) Mean current/voltage (*I*/*V*) relationships from control (triangles) and *ZmALMT1*-expressing oocytes (circles) recorded in the absence (open symbols) or presence (filled symbols) of Al^{3+}. The arrow indicates the 'indentation' of the current/voltage relationship resulting from the observed differences in inactivation of the inward currents at negative holding potentials as described in (c).

(c) Representative traces illustrating the partial deactivation of inward currents mediated by ZmALMT1. Currents shown correspond to those elicited between −150 and −90 mV in response to 10 mV steps, following the voltage protocol described in (a) (note the different time scales).

(d) Voltage dependence of deactivation time constants for ZmALMT1-mediated currents. Values shown represent the average λ_2 of at least seven independent measurements from oocytes of three donor frogs.

In order to elucidate the identity of the inward and outward currents mediated by ZmALMT1, we examined the current/voltage relationships recorded prior to and following addition of Al^{3+} to the bath medium when a source of organic acid was provided by pre-injecting the cells with citrate (Figure 8a) or malate (Figure 8b). Increasing the intracellular citrate or malate concentration to about 10 mM (based on an oocyte diameter of 1 mm) in ZmALMT1-expressing cells yielded current/voltage relationships similar to those observed in cells that were not pre-loaded with either organic acid. Addition of Al^{3+} to the bath medium resulted in the same small enhancement of the currents seen in cells not loaded with malate or citrate. The increase in intracellular citrate or malate concentration did not result in a significant shift in the reversal potential (i.e. the voltage at which the net current equals zero). Figure 8(c) compares the magnitude of the elicited currents under the various internal ionic conditions. The magnitude of the currents obtained when cells were pre-loaded with citrate and malate was slightly greater than those recorded in non-pre-loaded cells. Although such an increase in conductivity (i.e. current magnitude) upon increasing the intracellular anion concentration could be consistent with ZmALMT1 being capable of mediating citrate and malate efflux, the lack of a significant shift in the reversal potential upon varying the intracellular organic anion concentration indicates that ZmALMT1 is not permeable to either organic acid anion tested. Alternatively, if ZmALMT1 is in fact permeable to these organic anions, it is permeable in a non-selective way, as it cannot discriminate between these and other endogenous anions present in the oocyte's cytosol. Further characterization was performed by sequential replacement of the ions in the extracellular solution. Replacement of NaCl by choline-Cl did not result in any noticeable change in either the magnitude of the inward or outward ZmALMT1-mediated currents, or in the E_{rev} of the current, indicating that Na^+ is not the ion underlying the current mediated by ZmALMT1 (Figure 8d), and, as such, it is quite likely that the ZmALMT1-meditated currents are due to the influx and efflux of anions. Likewise, ZmALMT1-mediated currents were insensitive to changes in extracellular pH. It is worth noting that when cells were pre-loaded with citrate, the 'fingerprint' kinetics described previously for ZmALMT1 (i.e. the indentation in the *I*/*V* curves at around −100 mV) were not present (Figure 8a); however, this 'fingerprint' was observed when the cells were pre-loaded with malate or not pre-loaded at all (Figures 7b and 8b). These results suggest that, as in the case of rapidly activating (R-type) and Al^{3+}-activated plasma membrane anion channels (Piñeros and Kochian, 2001; Roberts, 2006), intra- or extracellular anions can regulate and modulate the voltage-dependent gating properties of ZmALMT1.

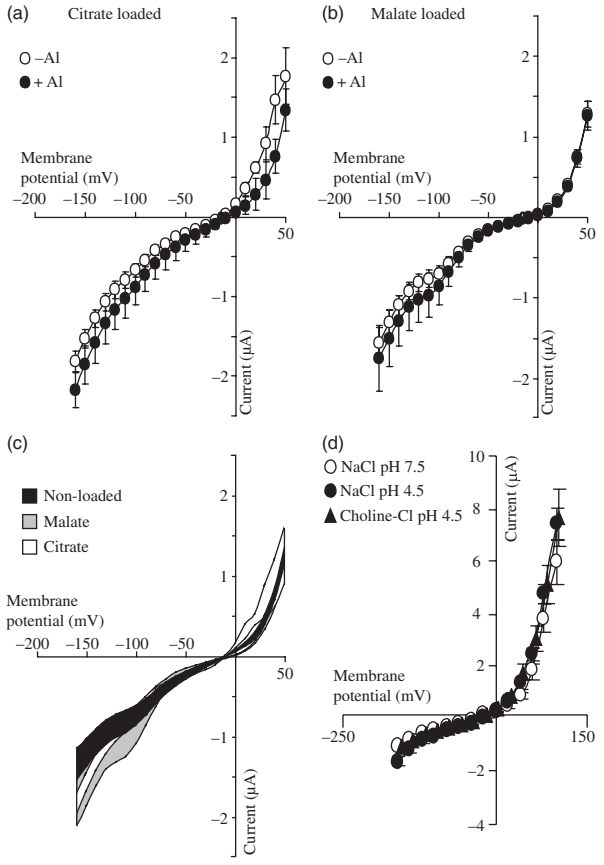

Figure 8. Identity of the ZmALMT1-mediated currents.
(a, b) Mean *I*/*V* relationships for *ZmALMT1*-expressing oocytes recorded in the absence (open symbols) or presence (filled symbols) of Al^{3+} in cells pre-loaded with (a) citrate or (b) malate. Currents are shown after subtraction of background currents determined in the respective control cells (i.e. currents from non-expressing cells pre-loaded with citrate or malate recorded in the presence and absence of Al^{3+}).
(c) *I*/*V* relationships comparing current magnitudes and reversal potentials (E_{rev}) recorded for *ZmALMT1*-expressing cells pre-loaded with water (black), citrate (white) or malate (gray) cells in the presence of Al^{3+}. The shaded area represents the mean current ± SEM calculated from at least 15 cells under each ionic condition.
(d) Mean *I*/*V* relationships from *ZmALMT1*-expressing oocytes recorded in a solution containing 96 mM NaCl (i.e. ND96) at pH 4.5 (open circles), pH 7.5 (filled circles) or in a solution where NaCl was replace by 96 mM choline-Cl (pH 4.5). Note that the voltage test pulses were between −160 and +100 mV (in 20 mV increments), resulting in significantly large positive currents. Consequently the *x* and *y* axis scales are different to those in (a)–(c).

Additional experiments were performed to further investigate the selectivity and conductivity properties of the current mediated by ZmALMT1 and elucidate the probabale functions of this protein *in planta* under abiotic stress conditions. We examined the *I*/*V* relationships from cells that were not pre-loaded with any organic acid and were subjected to extracellular solutions varying in Cl^- activity (the only anion present in the bath solution). Lowering extracellular [Cl^-] resulted in a concentration-dependent reduction in the magnitude of the ZmALMT1-mediated outward current, while the inward currents remained relatively unchanged (Figure 9a,b). In addition, the reversal potential of ZmALMT1-mediated currents became more positive as the extracellular [Cl^-] was lowered, consistent

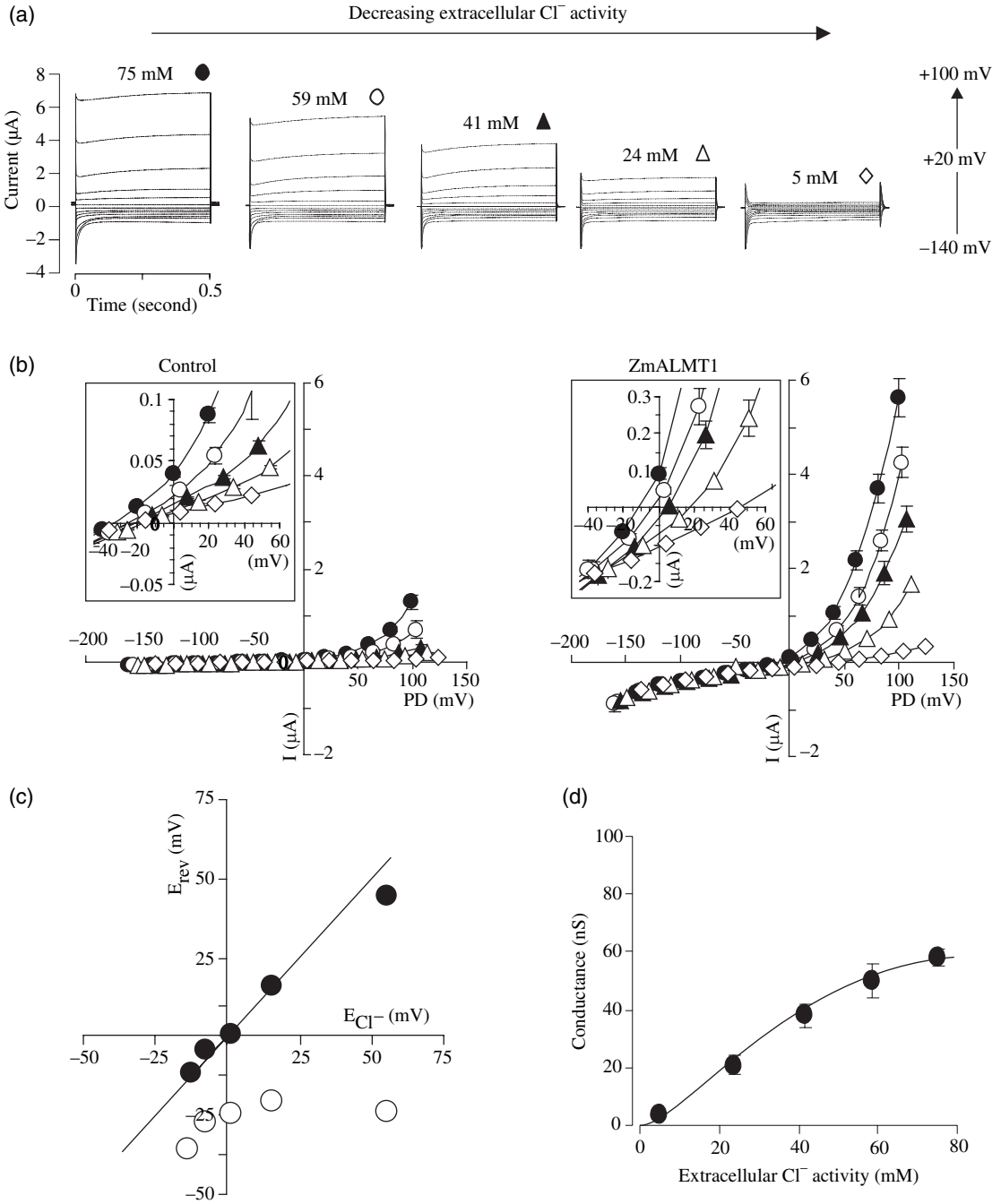

Figure 9. Anion selectivity of ZmALMT1.

(a) Example of ZmALMT1-mediated currents recorded from oocytes for a range of extracellular Cl^- activities as indicated on top of each set of traces. The holding potential was set to 0 mV, and voltage test pulses were stepped between −160 and +100 mV (in 20 mV increments). A 10 sec resting interval was allowed between successive voltage steps.

(b) Mean *I*/*V* relationships for control (left panel) and *ZmALMT1*-expressing oocytes (right panel) from recordings as described in (a). The extracellular Cl^- activity corresponds to the symbols shown in (a). The inset for each curve highlights the range of potentials (−40 to 60 mV) where the currents reversed (E_{rev}).

(c) E_{rev} from control (open circles) and *ZmALMT1*-expressing (closed circles) cells plotted as a function of the Cl^- equilibrium potential (E_{Cl^-}). E_{rev} values were calculated from those values shown in the insets to (b). The line represents values where E_{Cl^-} equals E_{rev}, assuming an internal Cl^- activity of 55 mM.

(d) Effect of extracellular Cl^- on the conductance (*G*) of the outward ZmALMT1-mediated currents. The conductance was estimated by linear regression of the four most positive test potentials from the *I*/*V* relationships shown in (b) (right panel) after the endogenous currents recorded in control cells had been subtracted.

with mineral anion transport underlying the ZmALMT1-mediated currents. Analysis of the ZmALMT1-mediated currents under these varying conditions revealed a close relationship between the theoretical E_{Cl^-} and the E_{rev} (Figure 9c). Given that the solutions only varied in their NaCl concentration, and that the E_{rev} values closely followed E_{Cl^-} (distant from the electrochemical equilibrium potential of Na^+), Cl^- was the major ion carrying the ZmALMT1-mediated currents under this set of ionic conditions. Figure 9(d) illustrates the effect of extracellular [Cl^-] on the conductance of the anion outward current (i.e. anion influx) mediated by ZmALMT1. The latter results indicate that, in contrast to the lack of permeation/selectivity observed for malate and citrate (as indicated by the lack of shift in E_{rev} upon loading the cells with these organic anions), ZmALMT1 can mediate anion (i.e. Cl^-) influx and efflux in a selective manner. The permeability of ZmALMT1 to other physiologically relevant anions was also evaluated by replacing the outside solution with an identical solution containing nitrate or sulfate (Figure 10). Addition of 10 mM NO_3^- or SO_4^{2-} did not result in any significant changes in the outward currents (i.e. anion influx) recorded from control cells. In contrast, cells expressing ZmALMT1 showed a significant increase in the outward currents upon addition of nitrate or sulphate. The larger (relative to control cells) outward current conductance recorded in ZmALMT1-expressing cells under conditions where the bath medium contained nitrate or sulfate is indicative of this transporter having the ability to transport a variety of mineral anions in addition to Cl^-.

Overall, the functional analysis of ZmALMT1 suggests that this transporter is involved in the selective transport of mineral anions. Given its low selectivity/conductivity for organic acids (in comparison to other mono- and divalent anions) and it expression profile (low expression at the root tip, in comparison to expression in the mature root and shoots), we conclude that ZmALMT1 is probably involved in mediating mineral nutrition and ion homeostasis processes, rather than playing an active role in mediating the specific Al-activated citrate exudation response at the root tip of maize roots.

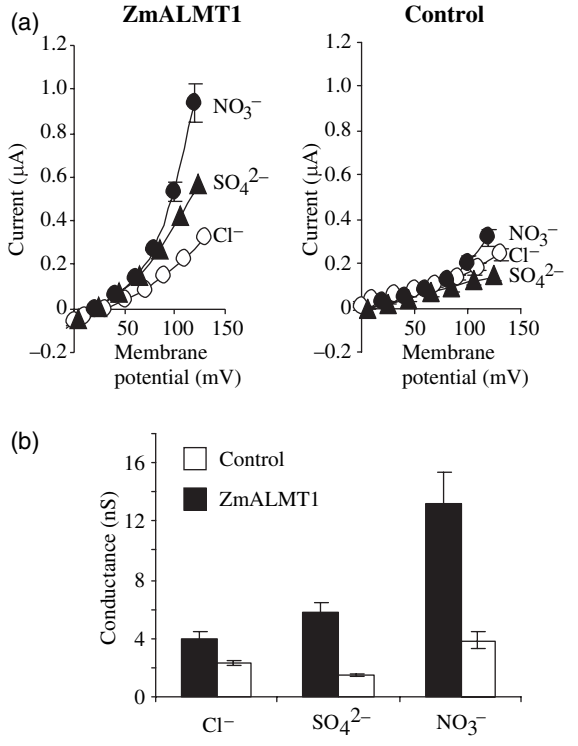

Figure 10. ZmALMT1 permeability to monovalent and divalent anions.
(a) Mean *I*/*V* relationships of the outward currents recorded from *ZmALMT1*-expressing oocytes bathed in a solution containing 5 mM Cl^- (open circles) plus 10 mM NO_3^- (closed circles) or SO_4^{2-} (closed triangles). The *I*/*V* relationships obtained for control cells under identical ionic conditions are shown on the right.
(b) Comparison of the outward current conductance recorded in control and *ZmALMT1*-expressing cells under the same ionic conditions as in (a). The conductance was estimated by linear regression of the four most positive test potentials from the *I*/*V* relationships shown in (a).

Discussion

The ALMT1 homologues functionally characterized so far from various plant species are structurally similar (Figure 4). The highly conserved N-terminal transmembrane domains are presumably responsible for forming the pore structure (i.e. permeation pathway), while the more variable hydrophilic C-terminal long tail is probably involved in regulation of these transporters. The latter is inferred from sequence analyses indicating that the C-terminal tail contains a number of serine, threonine and tyrosine residues that have a high probability of being phosphorylated (Iakoucheva *et al.*, 2006). These predictions are consistent with the observation that Al-activated malate efflux in wheat roots is inhibited by the kinase inhibitor K-252a, suggesting that protein phosphorylation is involved in activation of the malate efflux machinery by Al^{3+}, which could involve direct phosphorylation of the ALMT1 protein (Osawa and Matsumoto, 2001). Furthermore, a weak functional voltage dependence of ZmALMT1 suggests the existence of additional regulatory mechanisms. Interestingly, amino acid sequence alignments indicate a considerably higher degree of sequence identity between the wheat (TaALMT1) and maize (ZmALMT1) proteins relative to the Arabidopsis (AtALMT1) and rape (BnALMT) proteins. This contrasts with the higher degree of functional similarity in terms of Al activation and ion permeation (i.e. organic acid anion conductivity and selectivity) observed between TaALMT1 and AtALMT1 when compared to ZmALMT1.

Differences in the degree to which Al can regulate gene expression and/or directly activate the proteins are probably correlated with the role that each ALMT1 homologue plays in the organic acid release response. The almost instanta-

neous (e.g. wheat, buckwheat and maize) or delayed (e.g. *Cassia tora*) Al-activated organic acid efflux responses observed in various plant species upon exposure to Al have led to the proposition of alternative Al resistance patterns named I and II by Ma *et al.* (2001). In cases where rapid Al-activated root malate release occurs, all the cellular machinery (i.e. ALMT1-type transporters) necessary to mediate organic acid efflux is likely to be constitutively expressed, and exposure to Al solely activates the pre-existing cellular machinery. In wheat, *ALMT1* is in fact constitutively expressed, and activity of this transporter seems to be exclusively dependent on the presence of extracellular Al^{3+} (Sasaki *et al.*, 2004). Al^{3+} activation of TaALMT1 *in vitro* as well as the Al^{3+}-activated anion currents observed in wheat root protoplasts are strictly dependent on the presence of extracellular Al^{3+} (Ryan *et al.*, 1997). In the case of maize, although *ZmALMT1* is constitutively expressed at very low levels, the presence of Al^{3+} is not essential for activation of the ZmALMT1 transporter, and Al^{3+} only weakly enhances its transport activity *in vitro*.

Delays in the root organic acid exudation response that take place following exposure to Al have been interpreted as a requirement for up-regulation by Al of genes encoding transporters involved in anion efflux, with subsequent involvement (or not) of Al in regulating protein (e.g. transport) activity. Arabidopsis *AtALMT1* falls within this category; as *AtALMT1* gene expression is strongly upregulated by Al. The AtALMT1 protein is able to mediate a small malate efflux in the absence of Al, and Al exposure elicits a strong enhancement in malate efflux (Hoekenga *et al.*, 2006). Therefore, ZmALMT1 shares some similarities to AtALMT1, in that both their expression and transport activity are enhanced by Al^{3+}. Likewise, both transporters have intrinsic properties that allow them to mediate anion transport in the absence of Al^{3+}. However, it should be noted that the anion efflux mediated by ZmALMT1 is only weakly enhanced by Al, while AtALMT1 transport activity responds quite strongly to Al exposure. These results suggest that these ALMT1-type transporters require different triggering elements for Al^{3+} activation.

In terms of permeation characteristics, the phenotypes conferred by the various ALMT1 homologues expressed in *Xenopus* oocytes (Hoekenga *et al.*, 2006; Ligaba *et al.*, 2006; Sasaki *et al.*, 2004, and the present study) are in agreement with the finding that the *ALMT1*-like gene family encodes anion permeases. Although structurally similar, significant differences in the permeation properties of these transporters are starting to emerge, in addition to the distinct regulatory properties described above. Wheat ALMT1 and Arabidopsis AtALMT1 have a high selectivity for malate over other anions (Hoekenga *et al.*, 2006; Sasaki *et al.*, 2004), in agreement with the higher permeability of $malate^{2-}$ anions over Cl^- ($P_{mal}/P_{Cl^-} > 2.6$) reported previously for Al^{3+}-activated anion channels recorded in wheat root protoplasts (Zhang *et al.*, 2001). However, anion transport mediated by ZmALMT1 was insensitive to changes in internal malate or citrate, showing that these organic acids are unlikely to permeate ZmALMT1, and, if they do, they do so in a non-selective manner. The poor organic acid selectivity of ZmALMT1, especially when compared to other ALMT1-type transporters, agrees with the properties described for some other endogenous Al^{3+}-activated anion channels reported in maize root protoplasts, which, although permeable to citrate and malate [the selectivity sequence based on the magnitude of anion efflux currents was Cl^- (1.00) >> malate (0.28) > citrate (0.17); Kollmeier *et al.*, 2001], poorly discriminated for these ions over other predominant anions such as Cl^-.

The complexity of the transporters involved in Al-activated anion transport in maize root cells is just starting to be unraveled. The currents mediated by ZmALMT1 *in vitro* show rapidly/instantaneously activating inward current kinetics that resemble those described for endogenous Al^{3+}-activated plasma membrane channels in maize root protoplasts (Kollmeier *et al.*, 2001; Piñeros and Kochian, 2001; Piñeros *et al.*, 2002). Those studies have identified at least two types of Al-activated anion channels in various maize genotypes, with significant differences in their biophysical and regulatory properties (e.g. activation and deactivation kinetics). For example, Al-dependent anion channels studied by Kollmeier *et al.* (2001) in the maize genotype ATP-γ showed large transport rates (i.e. large unitary conductance), and differed in their activation (i.e. did not inactivate upon removal of Al^{3+}) and regulatory properties (i.e. were insensitive to changes in the extracellular anion) compared with Al-activated anion transporters from the maize genotypes SA3 and Cateto-Colombia (Piñeros and Kochian, 2001; Piñeros *et al.*, 2002). Differences in Al responsiveness as well as in the time lag between Al exposure and channel activation emphasize the possibility that more than one type of transporter may co-exist and be involved in organic acid efflux-mediated Al resistance in different maize genotypes.

The two maize genotypes chosen for this study contrast in their degree of Al resistance, and a strong association between higher Al-activated citrate exudation rates, Al exclusion and resistance was observed in the Al-resistant genotype Cat100-6 (Figure 1). These genotypes also differed in the magnitude of the Al-activated depolarization of the root cell membrane potential (E_m) observed in root tips (Figure 2). In fact, comparable genotypic differences in root cell E_m depolarization in response to Al have also been reported between Al-sensitive and Al-resistant wheat genotypes (Wherrett *et al.*, 2005). Although unlikely, these differences could result from differential blockade of Ca^{2+} and K^+ channels by Al^{3+} (Piñeros and Kochian, 2001; Piñeros and Tester, 1995, 1997) or by inhibition of the H^+-ATPase-derived proton motive force by Al^{3+} (Ahn *et al.*, 2002). Alternatively, these differences could be a result of differences in the

magnitude of anion efflux (e.g. Cl^- and ionized organic acids such as citrate) from root cells. Although ZmALMT1 functions as an anion transporter, its distinct functional properties (ion selectivity) revealed in oocytes argue against involvement of this transporter in the large Al-activated root citrate efflux observed in the tolerant maize genotype. Transport studies in oocytes revealed that, although ZmALMT1 is an anion-selective transporter, it is not an organic acid-specific transporter. The insignificant enhancement of anion transport activity by Al, being quite distinct from the large enhancement of malate efflux described for TaALMT1, AtALMT1 and BnALMT1 in response to Al, suggests that ZmALMT1 is not involved in Al-activated citrate release. In addition, the fact that expression of ZmALMT1 is low in root tips and equally upregulated by Al in both genotypes also argues against its role in the genotypic differences in Al-activated citrate exudation. The low constitutive *ZmALMT1* expression levels observed in root tips relative to the mature root and shoot tissues, together with its functional (i.e. selectivity) properties, suggest that ZmALMT1 is probably involved in mediating other mineral nutrition and ion homeostasis processes. These observations support the hypothesis that ZmALMT1 is not likely to be a major gene underlying Al resistance in maize.

The present results suggest that ZmALMT1, although quite similar in sequence to the ALMT1 transporters shown to play a major role in wheat, Arabidopsis and rape Al resistance, is substantially different in function from these ALMT1 transporters. Nevertheless, the greater Al-activated root citrate exudation observed in Al-tolerant Cat100-6, together with the lack of differences in root tip citrate concentration observed between Cat100-6 and S1587-17 (data not shown), are consistent with Al resistance in Cat100-6 being associated with organic acid transport rather than synthesis (Piñeros *et al.*, 2005). In addition, the differences observed in short-term Al responses (i.e. larger plasma membrane depolarization in Cat100-6 roots; Figure 2) suggest that structural and/or expression differences in a transporter mediating root citrate efflux could be a key aspect of the differential Al resistance in these maize genotypes. However, ZmALMT1 is not likely to be this transporter.

Consequently, an unidentified ALMT1-type transporter in maize may potentially underlie this response. In fact, in other plant species such as Arabidopsis, ALMT1 defines a gene family. Likewise, it is tempting to speculate that the diversity of the regulatory and functional properties of ALMT1-type proteins arises from their putative multi-subunit structure assembly. Although currently there is no biochemical/biophysical evidence supporting multimerization of subunits in any ALMT1-type transporter, this type of protein–protein interaction has been documented for several animal and plant membrane transporters. In fact, functional diversity by multimerization of subunits has been demonstrated in animal channels (Jan and Jan, 1990). Consequently, the formation of ALMT1-type hetero-multimeric structures could potentially generate functional diversity (i.e. changes in permeation/selectivity and regulation), conferring distinct roles for these ALMT protein complexes *in planta*. The latter would depend on the relative expression levels of each subunit. It is also plausible that organic acid transporters from other families may be involved in the maize Al-activated citrate exudation response. Transporters from the multi-drug and toxin efflux (MATE) family have recently been shown to mediate citrate transport in roots (Durrett *et al.*, 2007). Recently, a member of the MATE family encoding an Al-activated citrate efflux transporter was shown to underlie Al tolerance in sorghum (Magalhaes *et al.*, 2007). As sequencing of the maize genome progresses, it will be interesting to search for possible new candidates that might underlie the Al-activated organic acid exudation in the maize root tip. Furthermore, recent genetic and physiological evidence suggests that, unlike other cereals such as wheat and barley, Al resistance in maize is a genetically and physiologically complex trait, and, as such, Al-activated root citrate release may be only one of several Al resistance mechanisms contributing to maize Al resistance (Ninamango-Cárdenas *et al.*, 2003; Piñeros *et al.*, 2005).

Possible roles for ZmALMT1 in plant mineral nutrition

All of the ALMT1-type transporters functionally characterized prior to the present study mediate an Al-activated organic anion efflux, suggesting that they play a role in reducing the bioavailability of toxic Al^{3+} at the rhizosphere. The similar biophysical properties for the wheat ALMT1 and Al^{3+}-activated anion channels previously recorded from wheat root tips (Ryan *et al.*, 1997; Zhang *et al.*, 2001) indicate that ALMT1 is likely to mediate these endogenous currents. In contrast, the expression patterns and functional characteristics described here for ZmALMT1 suggest that this transporter does not underlie the Al^{3+}-activated endogenous currents reported in maize root cells (Kollmeier *et al.*, 2001; Piñeros and Kochian, 2001; Piñeros *et al.*, 2002). Rather, our results indicate that ZmALMT1 is a plasma membrane, anion-selective transporter that is predominantly expressed in the mature root, and is more likely to play a role in regulating inorganic anion transport. The transport of anions from the rhizosphere into the vascular tissue and their subsequent translocation involve the influx and efflux of anions across the plasma membrane of several distinct cell types. In fact, plasma membrane anion channels capable of mediating selective anion efflux and/or influx (similarly to ZmALMT1) have been identified in several types of root cells in various plant species. Outward currents (i.e. anion influx) have been reported in cells of

the root cortex in wheat (Garrill *et al.*, 1996; Skerrett and Tyerman, 1994) and maize (Piñeros and Kochian, 2001; Piñeros *et al.*, 2002), as well as in root epidermal cells in Arabidopsis (Diatloff *et al.*, 2004). Likewise, channels mediating inward currents (i.e. anion efflux) have been described in cells from the root periphery in maize (Piñeros *et al.*, 2002) and Arabidopsis (Diatloff *et al.*, 2004), and in cells from vascular tissues such as the stele (Gilliham and Tester, 2005) and xylem parenchyma (Kohler and Raschke, 2000; Kohler *et al.*, 2002) in barley and maize roots, respectively. It is worth noting that ZmALMT1 shares a number of functional similarities with some of these transporters. For example, its kinetics resemble those of the 'quickly activating anion conductance' described in maize root stelar cells (at hyperpolarized voltages, rapid activation of the current is followed by partial inactivation). However, its permeation properties resemble those described for anion channels in epidermal cells of Arabidopsis roots, which are also permeable to SO_4^{2-}, Cl^- and NO_3^-, but impermeable to malate and citrate. In addition, we cannot rule out the possibility of ZmALMT1 being permeable and selective to other organic anions not tested in the present study. However, ZmALMT1 is unlikely to mediate the flux of such substrates given its poor selectivity/permeability to malate and citrate. The functional similarities between ZmALMT1 and other anion channels described in plant root cells suggest that it may play a role similar to those proposed for some of these anion channels.

Overall, we propose that ZmALMT1 plays a role in anion homeostasis and mineral nutrition, similar to that described for other anion channels in higher-plant roots (see Roberts, 2006 and reference therein). Given the predominantly negative resting membrane potentials and the larger cytosolic anion (i.e. Cl^- and NO_3^-) concentrations in relation to extracellular anion concentrations found *in planta*, the anion electrochemical gradient favors passive efflux of anions from root cells. Given that ZmALMT1 mediates significantly large outward/inward currents, one possible physiological role for this transporter could be in loading and unloading anions into the xylem, provided that it localizes to cells of the inner root tissues (e.g. xylem parenchyma and/or stelar cells). On the other hand, if ZmALMT1 is localized to the root periphery (e.g. cortex and epidermal cells), it is unlikely to mediate the influx of anions from the rhizosphere into the root, given the unfavorable electrochemical gradient. Rather, it might function as an anion release mechanism, preventing the toxic accumulation of anions in the cytosol, and/or in the fine regulation of cytosolic anion concentrations. Alternatively, ZmALMT1-modulated Cl^- fluxes across the root cell plasma membrane could be involved in osmoregulation. Future investigations, including the tissue and cellular localization of *ZmALMT1* expression and gene expression studies in response to changes in plant mineral status and other abiotic stresses, are required to more clearly delineate the specific role(s) of ZmALMT1 in plant mineral nutrition processes.

Experimental procedures

Plant material and seedling growth

The maize (*Z. mays*) genotypes Cateto 100-6 (Al-resistant) and S1587-17 (Al-sensitive) (Moon *et al.*, 1997) were supplied by the Centro de Biologia Molecular e Engenharia Genética at the Universidade Estadual de Campinas (CBMEG–UNICAMP, Campinas, Brazil). Seeds were germinated and grown as previously described (Piñeros *et al.*, 2002, 2005).

Determination of root growth, organic acid exudation and Al content

Root growth measurements were made prior to and during the 5-day Al treatment at 24 h intervals. Relative root growth (RRG) was calculated as: RRG = RGR in solution containing 39 μM Al^{3+}/RGR in control solution, where RGR (root growth rate) = final root length – initial root length. Root exudates were collected in a simple salt solution after 24 and 48 h of exposure to Al^{3+} as described previously (Piñeros *et al.*, 2002, 2005) with the following modifications. Root exudates were collected only from the first 10 mm of the root of intact seedlings to avoid the potentially confounding effects of wounding observed in excised roots (Collet *et al.*, 2002). Removal of excess Cl^- from the exudates was performed using an OnGuard-Ag chromatography column (Dionex; http://www.dionex.com). Samples were then treated with cationic resin (Sigma-Aldrich, http://www.sigmaaldrich.com/) to remove excess Al^{3+} and other cations, lyophilized and resuspended in 1 ml 18 MΩ H_2O. Organic acid determinations were performed using a PACE 5510 capillary electrophoresis (CE) system (Beckman Instruments; http://www.beckmancoulter.com), under the conditions previously described (Piñeros *et al.*, 2002). Root Al content determinations were performed on the first centimeter of the root tips of seedlings. Roots were washed four times in 18 MΩ for a total of 1 h. Root tips were collected and dried in an oven at 55°C. Dry weights were determined using a microgram balance (MT2, Mettler Inc.; http://www.us.mt.com). Dry samples were then digested with 100 μl 70% perchloric acid, resuspended in 2 ml of 0.5% nitric acid, and analyzed using an ICP model 51000 emission spectrometer (Perkin-Elmer/Sciex; http://www.perkinelmer.com).

Cloning and sequencing of ZmALMT1

Genomic DNA was extracted from young leaves of the genotypes Cateto 100-6 and S1587-17 as described previously (Sambrook and Russell, 2001), and used as a template for PCR amplification using a set of primers designed based on the maize genomic sequence MAGI_92675 (http://www.plantgenomics.iastate.edu/maize). The PCR products obtained from each genotype (approximately 4.5 kb) were TA-cloned into the pCR2.1-TOPO vector (Invitrogen, http://www.invitrogen.com/) and fully sequenced using internal primers. *ZmALMT1* cDNA was obtained by amplifications using a pair of primers designed for the start and stop codons predicted from the MAGI and EST sequences. The PCR products obtained were TA-cloned into pCR2.1-TOPO (Invitrogen) and fully sequenced (Genbank accession number DQ358745). Secondary structure predictions for the of ZmALMT1 protein were carried out using TMpred (Hofmann

and Stoffel, 1993) and SOSUI algorithms (Hirokawa *et al.*, 1998). Motif elements were recognized using PROSITE (Rost *et al.*, 2003).

Semi-quantitative RT-PCR

Total RNA was extracted from root tips (10 mm), the rest of the root and from shoots using TRIzol reagent (Invitrogen) following the manufacturer's protocol. Prior to reverse transcription, RNA samples were treated with DNAse I for 15 min at room temperature; DNAse I was inactivated by incubation with 1 μl 25 mM EDTA at 65°C for 10 min. First-strand cDNA was synthesized from 3.5 μg of total RNA using SuperScript III reverse transcriptase (Invitrogen) and an oligo(dT)$_{20}$ primer at 50°C overnight. Reactions were terminated by incubation at 70°C for 15 min. The cDNA samples were used as templates in amplifications under standard conditions using internal primers for *ZmALMT1* (forward: 5-CTCTCGCTTC-CTACGTCATCACCCTC-3; reverse: 5-CTGAGGTCCTTGGCCGCTTT-GGCT-3) and for the *18S* loading control (forward: 5-TCGATT-CCGGAGAGGGAGCCTGAGA-3; reverse: 5-TGCTGGCACCAGACTT-GCCCTCCA-3). To determine optimal semi-quantitative conditions for the RT-PCR, samples were amplified and sampled at various points between 30 and 45 (for *ZmALMT1*) or 10 and 25 (for *18S*) cycles. Subsequent amplifications were performed at 38 cycles for *ZmALMT1* and 12 cycles for *18S*.

Localization of ZmALMT1 protein

Subcellular localization of the ZmALMT1 protein was determined via transient expression of a 35S:*ZmALMT1*::GFP translational fusion in onion (*Allium cepa*) epidermal cells. The 35S:*ZmALMT1*::GFP construct was generated as follows. The coding region of *ZmALMT1* (cDNA) was used as a template for amplification using adaptor primers that incorporated *Spe*I restriction sites for sub-cloning into the plant transformation vector, pCAMBIA1302. This vector contains the CaMV 35S promoter driving the *mGFP5* gene (accession number AF234298, http://www.cambia.org; Siemering *et al.*, 1996). Insertion of *ZmALMT1* into an *Spe*I site located between the 35S promoter and the GFP coding region generated a translational in-frame fusion of *ZmALMT1* and GFP driven by the 35S promoter. The resulting construct was fully sequenced and checked for sequence accuracy.

Transient expression of the *ZmALMT1*::GFP chimera was achieved by particle bombardment of epidermal onion cells. Briefly, M10 tungsten particles (1.1 μm) were coated with 2 μg of plasmid DNA (*ZmALMT1*::GFP chimera or empty pCAMBIA1302 as a negative control) using 2.5 M $CaCl_2$ and 1 M spermidine (Sigma). Epidermal onion peels were bombarded at a helium pressure of 9 MPa (biolistic PDS-1000/He; BioRad Laboratories, http://www.bio-rad.com/) with the DNA-coated particles, and the tissue was incubated on filter paper immersed in tap water in the dark at room temperature for 24 h. Documentation of GFP fluorescence was carried out using confocal microscopy (Leica TCS SP2 system; http://www.leica-microsystems.com).

Root membrane potential measurements in maize roots

Measurements of the electrical potential difference (E_m) across the maize root cell plasma membrane were recorded using a glass microelectrode (tip diameter ≤1 μm). The seminal roots of intact maize seedlings were pre-treated for 24 h in 200 μM $CaCl_2$ (pH 4.5), placed in a recording chamber, fixed horizontally with small acrylic blocks and silicon grease, and constantly bathed with control solution (200 μM $CaCl_2$, pH 4.2). Roots were allowed to equilibrate for 10–15 min before impalement. The flow rate of the bathing solution was kept constant during the entire recording at approximately 4 ml min^{-1}. The impaling microelectrode was filled with 3 M KCl (adjusted to pH 2.0 with HCl to reduce tip potentials), and the E_m was recorded using a model FD 223 amplifier (World Precision Instruments Inc.; http://www.wpiinc.com) and a single reference electrode placed in the bath solution. The output signal was continually digitized using a Digidata 1320A data acquisition system (Axon Instruments; http://www.axon.com). Following a stable measurement of E_m, the control solution was replaced by an identical solution containing 60 or 150 μM $AlCl_3$ (39 and 90 μM Al^{3+} activity, respectively). E_m recordings were obtained at two sites along the root: the first site was directly on the root apex, while the second was located 10 mm further back from the apex (elongation zone).

Expression of ZmALMT1 in *Xenopus* oocytes

cRNA was prepared using the RNA capping kit (Stratagene, http://www.stratagene.com/), according to the manufacturer's instructions, from *Nde*I-digested T7TS plasmid DNA containing the *ZmALMT1* coding region cloned from Cat100-6 flanked by the 3′ and 5′ UTRs of a *Xenopus* β-globin gene. The cRNA was divided into 1.5 μl aliquots and stored at −80°C until injection. Harvesting of stage V–VI *X. laevis* oocytes was performed as described previously (Golding, 1992). De-folliculated oocytes were maintained in ND96 solution (supplemented with 50 μg ml^{-1} gentamycin) at 18°C overnight prior to injections. Oocytes were injected with 48 nl of water containing 30 ng of cRNA encoding *ZmALMT1* (or 48 nl of water as a control), and incubated in ND96 at 18°C for 2–4 days. Whole-cell currents from oocytes expressing *ZmALMT1* were recorded under constant perfusion at room temperature (22°C) using a GeneClamp 500 amplifier (Axon Instruments) using conventional two-electrode voltage-clamp (TEVC) techniques. The output signal was digitized and analyzed using a Digidata 1320A Pclamp 9 data acquisition system (Axon Instruments). Recording electrodes filled with 0.5 M K_2SO_4 and 30 mM KCl had resistances between 0.5–1.2 MΩ. Recordings were performed in oocytes that were or were not preloaded with water, citrate or malate, by injecting 48 nl of water, 0.1 M sodium citrate or 0.1 sodium malate (all at pH 7.5), 2–4 h prior to impalement. Recordings were performed in several types of solutions. The main ND96 solution consisted of (in mM): 96 NaCl, 1 KCl, 1.8 $CaCl_2$ and 0.1 $LaCl_3$, with or without 0.1 $AlCl_3$ (pH 4.5), yielding an activity of 10 μM Al^{3+}. This Al^{3+} activity was the same as employed in the electrophysiological characterization of other ALMT1 homologues expressed in *Xenopus* oocytes (Hoekenga *et al.*, 2006; Ligaba *et al.*, 2006; Sasaki *et al.*, 2004). The solutions used in anion selectivity experiments had a similar ionic composition, except that extracellular Cl^- activity was adjusted to the desired value by decreasing the total NaCl in the solution (from 96 mM to 72, 48, 24 and 0 mM NaCl) while maintaining the $CaCl_2$ and KCl concentrations. The resulting solutions had total Cl^- activities of 75, 59, 41, 24 and 5 mM, respectively (as calculated by GEOCHEM; Parker *et al.*, 1995). The solutions used to test nitrate and sulphate permeation consisted of a solution lacking NaCl (i.e. 5 mM total Cl^-) as described above, with an additional 10 mM $NaNO_3$ or Na_2SO_4, with resulting NO_3^- and SO_4^{2-} activities of 8.4 and 4.3 mM, respectively. The pH of all solutions was adjusted to 4.5, and the Al^{3+} activity was maintained at 10 μM by addition of the corresponding $AlCl_3$ concentration, as determined by GEOCHEM (Parker *et al.*, 1995). The osmolarity of all solutions was adjusted to 195 mOsm kg^{-1} using sorbitol. Liquid junction potentials were measured and corrected according to the method described by Neher (1992). All potentials

given, including reversal potentials (E_{rev}), were corrected by off-line subtraction of the experimental junction potentials tested for each ionic condition. Currents were measured in response to voltage test pulses (400 or 500 msec in duration) between −160 to +50 mV (in 10 mV increments) or between −160 to +100 mV (in 20 mV increments) stepped from a holding potential set to 0 mV, with a 10 sec resting phase at 0 mV between each voltage pulse. The current/voltage (*I*/*V*) relationships measured under the various conditions were constructed by measuring the current amplitude at the end of the test pulses. Deactivation time constants were obtained by fitting the currents (for 100 msec following the capacitance spike) to a second-order exponential: $I = A_1 \cdot \exp(-t/\lambda_1) + A_2 \cdot \exp(-t/\lambda_2) + C$, where A_1 and A_2 are the amplitude, C is the current offset, and λ_1 and λ_2 are the time constants. All values are the means ± SEM for at least 10 cells recorded from four donor frogs.

Acknowledgements

The authors would like to thank Jon Shaff, Randy Clark, Eric Craft, Vera Alves, EMBRAPA Maize and Sorghum Research Center, Sete Lagoas, Brazil, and Jiping Liu for assistance during the development of this work. The authors would also like to thank two anonymous reviewers for their constructive comments on the manuscript. The project was supported by National Science Foundation (NSF) Plant Genome grant DBI 0419435 to L.V.K. G.M.A.C. was supported by scholarships from the Fundação de Amparo à Pesquisa do Estado de Minas Gerais (FAPEMIG, Brazil) and the Coordenação de Aperfeiçoamento de Pessoal de Nível Superior (CAPES, Brazil).

References

Ahn, S. J., Sivaguru, M., Chung, G. C., Rengel, Z. and Matsumoto, H. (2002) Aluminium-induced growth inhibition is associated with impaired efflux and influx of H+ across the plasma membrane in root apices of squash (*Cucurbita pepo*). *J. Exp. Bot.* **53**, 1959–1966.

Collet, L., De Leon, C., Kollmeier, M., Schmohl, N. and Horst, W. J. (2002) Assessment of aluminium sensitivity of maize cultivars using roots of intact plants and excised root tips. *J. Plant Nutr. Soil Sci.* **165**, 357–365.

Delhaize, E., Ryan, P. R., Hebb, D. M., Yamamoto, Y., Sasaki, T. and Matsumoto, H. (2004) Engineering high-level aluminum tolerance in barley with the ALMT1 gene. *Proc. Natl Acad. Sci. U.S.A.* **101**, 15249–15254.

Diatloff, E., Roberts, M., Sanders, D. and Roberts, S. K. (2004) Characterization of anion channels in the plasma membrane of Arabidopsis epidermal root cells and the identification of a citrate-permeable channel induced by phosphate starvation. *Plant Physiol.* **136**, 4136–4149.

Durrett, T. P., Gassmann, W. and Rogers, E. E. (2007) The FRD3-mediated efflux of citrate into the root vasculature is necessary for efficient iron translocation. *Plant Physiol.* **144**, 197–205.

Garrill, A., Tyerman, S. D., Findlay, G. P. and Ryan, P. R. (1996) Effects of NPPB and niflumic acid on outward K+ and Cl^- currents across the plasma membrane of wheat root protoplasts. *Aust. J. Plant Physiol.* **23**, 527–534.

Gilliham, M. and Tester, M. (2005) The regulation of anion loading to the maize root xylem. *Plant Physiol.* **137**, 819–828.

Golding, A. (1992) Maintenance of *Xenopus laevis* and oocyte injection. *Methods Enzymol.* **207**, 266–279.

Hirokawa, T., Seah, B. C. and Mitaku, S. (1998) SOSUI: classification and secondary structure prediction system for membrane proteins. *Bioinformatics*, **14**, 378–379.

Hoekenga, O. A., Maron, L. G., Piñeros, M. A. *et al.* (2006) AtALMT1, which encodes a malate transporter, is identified as one of several genes critical for aluminum tolerance in Arabidopsis. *Proc. Natl Acad. Sci. U.S.A.* **103**, 9738–9743.

Hofmann, K. and Stoffel, W. (1993) TMbase – a database of membrane spanning proteins segments. *Biol. Chem. Hoppe-Seyler*, **374**, 166.

Iakoucheva, L. M., Radivojac, P., Brown, C. J., O'Connor, T. R., Sikes, J. G., Obradovic, Z. and Dunlap, K. (2006) The importance of intrinsic disorder for protein phosphorylation. *Nucleic Acids Res.* **32**, 1037–1049.

Jan, L. Y. and Jan, Y. N. (1990) How might the diversity of potassium channels be generated? *Trends Neurosci.* **13**, 415–419.

Jorge, R. A. and Arruda, P. (1997) Aluminum-induced organic acids exudation by roots of an aluminum-tolerant tropical maize. *Phytochemistry*, **45**, 675–681.

Kochian, L. V., Hoekenga, O. A. and Piñeros, M. A. (2004) How do crop plants tolerate acid soils? Mechanisms of aluminum tolerance and phosphorous efficiency *Annu.Rev. Plant Biol.* **55**, 459–493.

Kochian, L. V., Piñeros, M. A. and Hoekenga, O. A. (2005) The physiology, genetics and molecular biology of plant aluminum resistance and toxicity. *Plant Soil*, **274**, 175–195.

Kohler, B. and Raschke, K. (2000) The delivery of salts to the xylem: three types of anion conductance in the plasmalemma of the xylem parenchyma of roots of barley. *Plant Physiol.* **122**, 243–254.

Kohler, B., Wegner, L. H., Osipov, V. and Raschke, K. (2002) Loading of nitrate into the xylem: apoplastic nitrate controls the voltage dependence of X-QUAC, the main anion conductance in xylem-parenchyma cells of barley roots. *Plant J.* **30**, 133–142.

Kollmeier, M., Dietrich, P., Bauer, C. S., Horst, W. J. and Hedrich, R. (2001) Aluminum activates a citrate-permeable anion channel in the aluminum-sensitive zone of the maize root apex. A comparison between an aluminum-sensitive and an aluminum-resistant cultivar. *Plant Physiol.* **126**, 397–410.

Ligaba, A., Katsuhara, M., Ryan, P. R., Shibasaka, M. and Matsumoto, M. (2006) The BnALMT1 and BnALMT2 genes from *Brassica napus* L. encode aluminum-activated malate transporters that enhance the aluminum resistance of plant cells. *Plant Physiol.* **142**, 1294–1303.

Ma, J. F., Ryan, P. R. and Delhaize, E. (2001) Aluminium tolerance in plants and the complexing role of organic acids. *Trends Plant Sci.* **6**, 273–278.

Magalhaes, J. V., Liu, J., Guimarães, C. T. *et al.* (2007) A member of the multidrug and toxic compound extrusion 'MATE' family is a major gene that confers aluminum tolerance in sorghum. *Nature Genet.* **39**, 1156–1161.

Mariano, E. D. and Keltjens, W. G. (2003) Evaluating the role of root citrate exudation as a mechanism of aluminium resistance in maize genotypes. *Plant Soil*, **256**, 469–479.

Moon, D. H., Ottoboni, L. M. M., Souza, A. P., Sibov, S. T., Gaspar, M. and Arruda, P. (1997) Somaclonal-variation-induced aluminum-sensitive mutant from an aluminum-inbred maize tolerant line. *Plant Cell Rep.* **16**, 686–691.

Neher, E. (1992) Correction for liquid junction potentials in patch clamp experiments. *Methods Enzymol.* **207**, 123–131.

Ninamango-Cárdenas, F. E., Guimaraes, C. T., Martins, P. R., Parentoni, S. N., Carneiro, N. P., Lopes, M. A., Moro, J. R. and Paiva, E. (2003) Mapping QTLs for aluminum tolerance in maize. *Euphytica*, **130**, 223–232.

Osawa, H. and Matsumoto, H. (2001) Possible involvement of protein phosphorylation in aluminum-responsive malate efflux from wheat root apex. *Plant Physiol.* **126**, 411–420.

Parker, D. R., Norvell, W. A. and Chaney, R. L. (1995) GEOCHEM-PC: a chemical speciation program for IBM and compatible computers. In *Chemical Equilibrium and Reaction Models* (Loeppert, R. H., Schwab, A. P. and Goldberg, S., eds). Madison, WI: Soil Science Society of America, pp. 253–269.

Pellet, D. M., Grunes, D. L. and Kochian, L. V. (1995) Organic-acid exudation as an aluminum-tolerance mechanism in maize (*Zea mays* L). *Planta*, **196**, 788–795.

Piñeros, M. A. and Kochian, L. V. (2001) a patch-clamp study on the physiology of aluminum toxicity and aluminum tolerance in maize. identification and characterization of Al^{3+}-induced anion channels. *Plant Physiol.* **125**, 292–305.

Piñeros, M. and Tester, M. (1995) Characterization of a voltage-dependent Ca^{2+}-selective channel from wheat roots. *Planta*, **195**, 478–488.

Piñeros, M. and Tester, M. (1997) Calcium channels in higher plant cells: selectivity, regulation and pharmacology. *J. Exp. Bot.* **48**, 551–577.

Piñeros, M. A., Magalhaes, J. V., Alves, V. M. C. and Kochian, L. V. (2002) The physiology and biophysics of an aluminum tolerance mechanism based on root citrate exudation in maize. *Plant Physiol.* **129**, 1194–1206.

Piñeros, M. A., Shaff, J. E., Manslank, H. S., Alves, V. M. C. and Kochian, L. V. (2005) Aluminum resistance in maize cannot be solely explained by root organic acid exudation. A comparative physiological study. *Plant Physiol.* **137**, 231–241.

Raman, H., Zhang, K. R., Cakir, M. *et al.* (2005) Molecular characterization and mapping of ALMT1, the aluminium-tolerance gene of bread wheat (*Triticum aestivum* L.). *Genome*, **48**, 781–791.

Roberts, S. K. (2006) Plasma membrane anion channels in higher plants and their putative functions in roots. *New Phytol.* **169**, 647–666.

Rost, B., Yachdav, G. and Liu, J. (2003) The PredictProtein server. *Nucleic Acids Res.* **32**, W321–W326.

Ryan, P. R., Skerrett, M., Findlay, G. P., Delhaize, E. and Tyerman, S. D. (1997) Aluminum activates an anion channel in the apical cells of wheat roots. *Proc. Natl Acad. Sci. U.S.A.* **94**, 6547–6552.

Sambrook, J. and Russell, D. (2001) *Molecular Cloning: A Laboratory Manual*. Cold Spring Harbor, NY: Cold Spring Harbor Laboratory Press.

Sasaki, T., Yamamoto, Y., Ezaki, B., Katsuhara, M., Ahn, S. J., Ryan, P. R., Delhaize, E. and Matsumoto, H. (2004) A wheat gene encoding an aluminum-activated malate transporter. *Plant J.* **37**, 645–653.

Siemering, K., Golbik, R., Sever, R. and Haseloff, J. (1996) Mutations that suppress the thermosensitivity of green fluorescent protein. *Curr. Biol.* **6**, 1653–1663.

Skerrett, M. and Tyerman, S. D. (1994) A channel that allows inwardly directed fluxes of anions in protoplasts derived from wheat roots. *Planta*, **192**, 295–305.

Tusnady, G. E. and Simon, I. (2001) The HMMTOP transmembrane topology prediction server. *Bioinformatics*, **17**, 849–850.

Wherrett, T., Ryan, P., Delhaize, E. and Shabala, S. (2005) Effect of aluminum on membrane potential and ion fluxes at the apices of wheat roots. *Funct. Plant Biol.* **32**, 199–208.

Yamaguchi, M., Sasaki, T., Sivaguru, M., Yamamoto, Y., Osawa, H., Ahn, S. J. and Matsumoto, H. (2005) Evidence for the plasma membrane localization of Al-activated malate transporter (ALMT1). *Plant Cell Physiol.* **46**, 812–816.

Zhang, W. H., Ryan, P. R. and Tyerman, S. D. (2001) Malate-permeable channels and cation channels activated by aluminum in the apical cells of wheat roots. *Plant Physiol.* **125**, 1459–1472.

